Structural Optimization of Orifice Rotameter Based on CFD

Li-hua PIAO, Tao ZHANG
School of Electrical Engineering and Automation, Tianjin University, China;
No. 92, Wei Jin Road, Nan Kai District, Tianjin City, Tianjin 300072
Tel: 86-022-81287825, FAX: 86-022-27404274, E-mail: hbpiaolh@163.com

Tong GUO, Xiao-zhong Li, Xing CHEN
Tianjin Institute of Metrological Supervision and Testing, China;
Tel: 86-022-23009334, E-mail: gttjjl@126.com

Abstract： The orifice rotameter indicates the flowrate as a displacement of a symmetrical body(float) placed concentrically downstream of an orifice inside a vertical tube. Experiments study had been performed at five positions of the float to evaluate the performance of the most commonly used type of orifice rotameter. The computational fluid dynamics (CFD) method was employed to optimize the performance of orifice rotameter. A total of 20 numerical models were established corresponding to the five positions, four types of orifice rotameter. At the same position, the floats of four types of numerical models have the same stroke with experimental flowmeter. Numerical models of 3D turbulence flow field of the orifice rotameter were conducted. The error analysis method of the float forced balance, which controls the computational precision, was adopted to adjust the inlet flowrate. The results of numerical calculation showed that new types of orifice rotameter improved the flow stability and linearity. The paper described the design and results to verify the performance of the new kinds of orifice rotameter.

Keywords: orifice rotameter, experiments study, computational fluid dynamics, numerical models, flow stability and linearity

1. Introduction

Owing to simple structure, small pressure loss and stable performance, particularly its robustness, the metal tube variable area flow meter (rotameter) holds a significant portion in the process control area. As shown in Fig. 1a, detection elements of the mental tube rotameter are composed of a vertical conical tube and a float moving along the cone center axis. It is often known as cone rotameter. Another structure is shown in Fig. 1b, which is often called orifice rotameter. Its detection elements are composed of an orifice and a

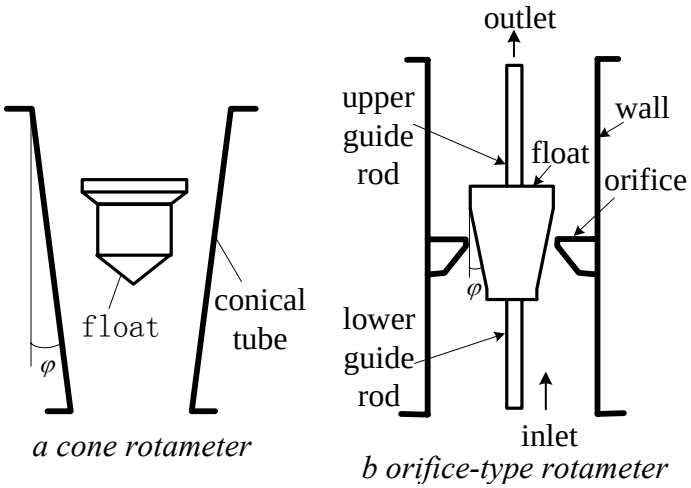

a cone rotameter *b orifice-type rotameter*

Fig.1 Structural figure of rotameter

float moving along the center axis of orifice. Orifice rotameter has simple structure, easy to process, widely used in recent years. It is easy machining that change the conical tube's inner cone angle φ of the cone rotameter to the float's outer cone angle φ of the orifice rotameter. But compared with cone rotameter, orifice rotameter has poor linearity and stability. Especially near the upper limit of range, it is very inconvenient for the user to reading because of large indication fluctuations.

The computational fluid dynamics (CFD) method was employed to optimize the performance of orifice rotameter. A total of 20 numerical models were established corresponding to the five locations of four types of orifice rotameter. At the same position, the floats of four types of numerical models have the same stroke with experimental flow meter. Numerical models of 3D turbulence flow field of the orifice rotameter were conducted. Not only CFD method can calculate the flow values of different location of float, but also can provide internal pressure distribution, velocity distribution, flow separation etc. It provides basis for the optimization of orifice rotameter.

2. Principle of Orifice Rotameter

The most commonly used type of orifice rotameter is shown in Fig. 1b.It indicates the flowrate as a displacement of the float placed concentrically downstream of an orifice inside a vertical tube. In order not to hit the wall when the float moves up and down along the orifice and to enhance the stability of the float, the guide bars were installed on the upper surface and lower surface of the float.

As shown in Fig. 2, the measured fluid passed upwards through the rotameter, which was inserted into the flow circuit. The forces imposed on the Float and the guide bar include differential pressure F_1, buoyancy force F_2 and gravitational force G. F_1 and F_2 constitute lift force F_S of the float and guide rods. If F_S is greater than G, the float was carried upwards by the passage of the fluid. With the float rising, the ring area between the float and the orifice increases, the flowrate decreases, and F_1 reduces. Corresponding the lift force F_S which acting on the float and guide rod reduces. The float reaches to a height h in the tube where its weight G is balanced by the force F_S. The displacement h is a measure of the volumetric flowrate q_v. For incompressible flow [1]

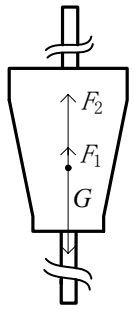

Fig. 2 The force imposed on float

$$q_v = \alpha\pi(D_f h \tan\varphi + h^2 \tan^2\varphi)\sqrt{\frac{2gV_f(\rho_f - \rho)}{\rho A_f}} \quad (1)$$

Where

A: flowrate coefficient, constant

D_f: the maximum diameter of float, m

g: local gravity acceleration, m / s^2

A_f: cross-sectional area of the float, m^2

V_f: float volume, m^3

ρ: fluid density, kg/m^3

ρ_f: float density, kg/m^3

3. Structure and Parameters

The key technical data of metal tube DN100 orifice rotameter (Orifice100) are as follows: flow measurement of liquids is water at 20 ℃, measuring span 10: 1, the upper limit of the range of volumetric flowrate is 63m^3/h, and measurement accuracy of the flowrate is ±1.5%. Fig.3 (a) shows the structure diagram of Orifice100. The main structural parameters are shown in Table 1. The three kinds of new structural type are shown in Fig.3 (b) ~ 3 (d). Except the values in Table.2, other parameters are the same with Fig.3 (a).

Table.1 Main structural parameters of Orifice100 mm

D_1	D_2	D_3	D_4	D_5	D_6	D_7	H_1	H_2	H_3	H_4	H_5	H_6	H_7
16	60	87	122	113	90	120	67	5	50	15	70	17	3

Table.2 Main structural parameters of new kind of orifice rotameter mm

Orifice100-1		Orifice100-2			Orifice100-3		
H_7	H_8	H_4	H_8	D_8	D_8	H_3	H_8
2	8	13	2	91	75	30	20

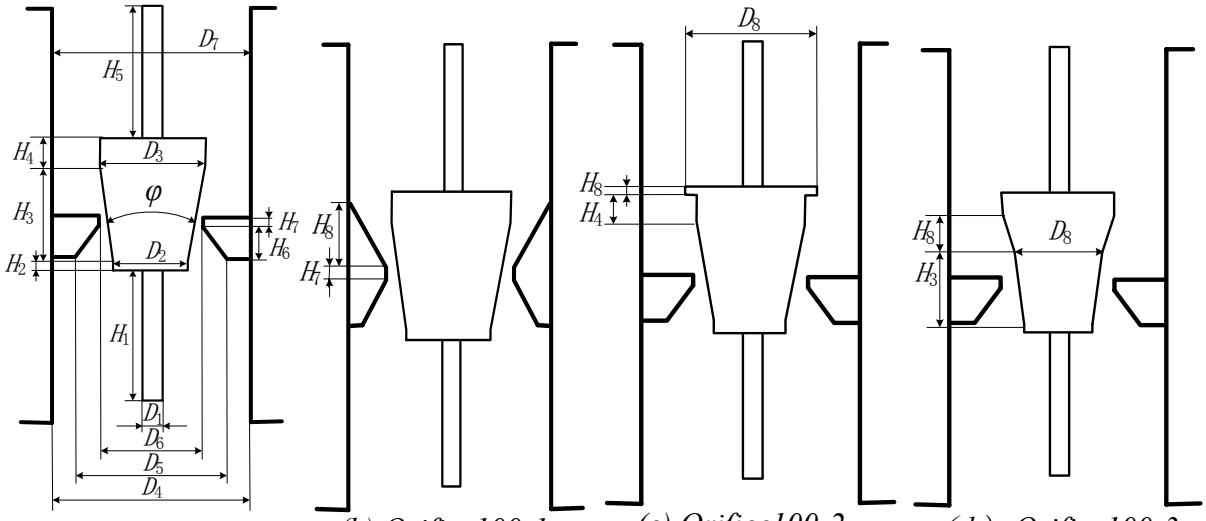

(a) Orifice100 (b) Orifice100-1 (c) Orifice100-2 (d) Orifice100-3

Fig.3 Structural parameters figure of DN100 orifice-type rotameter

4 Experimental Programme

To determine the float positions of CFD numerical models, experiments were done to get *h* corresponding to each flow points.

4.1 Experimental Facility

Fig.4 shows the water flow standard facility. The supply of water was obtained from a large overhead water tower situated at an elevation of approximately 32.5 m above the ground, which can continuously adjust the flow range. Gravimetric method and standard meter method can both be applied to calibrate the rotameter. The measurement uncertainty is 0.2%. During the tests, the bulk flowrate is determined by transfer standard. A turbine meter calibrated by weigh-time system was used to measure the test flowrate.

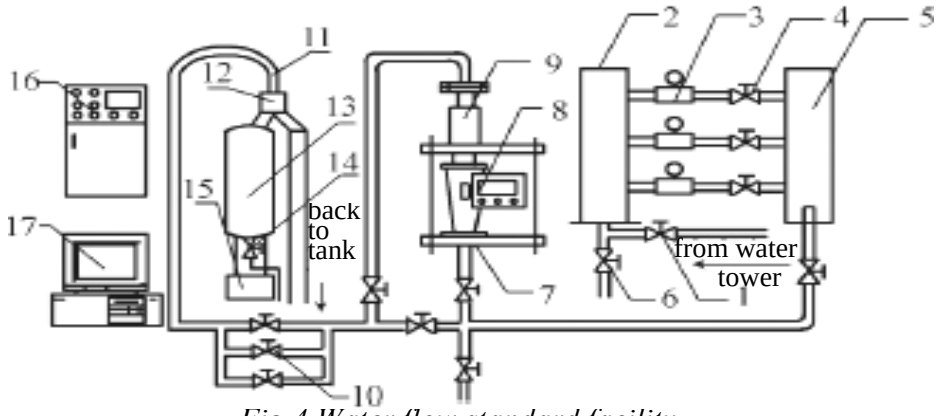

Fig.4 Water flow standard facility

1-inlet valve, 2-filter tank, 3-standard meter, 4-off valve, 5-balance tank, 6-discharge valve, 7-support plate; 8-rotameter, 9-device for clamping meter, 10-flow control valve, 11-nozzle, 12-commutator, 13-gauges, 14-release valve, 15-electronic scales, 16-control cabinet, 17-computer

4.2 Experimental Procedure

1) According to requirements of Reference [2], total 5 points (q_{min}, 0.25 q_{max}, 0.4 q_{max}, 0.7 q_{max} and q_{max}) of Orifice100 were selected to be tested on the experimental facility shown in Fig.4, where q_{min} is the lower limit of the range of volumetric flowrate and q_{max} is the upper limit of the range of volumetric flowrate.

2) To calculate the full-scale errors δ_{SF} of each flow points.

$$\delta_{SF} = (q_b - q_a) / q_{max} \times 100\ \% \quad (2)$$

Where

q_b: volumetric flowrate of standard meter, m^3/h

q_a: arithmetic mean volumetric flowrate of rotameter, m^3/h

q_{max}: the max volumetric flowrate of rotameter, m^3/h

3) To compute linearity using the least square method. The fitting line equation is $q_0 = a_0 + k \cdot h$, where q_0 represents ideal volumetric flowrate, m^3/h. Difference between the measured volumetric flowrate q_i and the ideal volumetric flowrate q_{0i} is $\triangle_i = q_i - q_{0i}$. So

$$k = \triangle_i / q_{max} \times 100\% \quad (3)$$

4.3 Experimental Data

As described in 3.2, Orifice100 was calibrated on the standard facility shown in Fig.4. The experiment data were shown in Table 3, where k_a is linearity of q_a calculated from equation (3).

Table.3 Experimental data of Orifice100

q_b/(m^3/h)	h/ mm	q_a/(m^3/h)	δ_{SF}/ %	k_a/ %
6.496	4.2	6.115	-0.605	8.92
15.699	18.2	15.735	0.057	
25.444	22.5	25.200	-0.387	
44.121	33.8	44.100	-0.033	
63.068	45.2	63.000	-0.108	

From Table 3 it can be seen that,

1) k_a of Orifice100 is 8.92%. It can be seen that the linearity of Orifice100 is poor.
2) The max δ_{SF} of Orifice100 is -0.605%.δ_{SF} can meet the precision requirement of ±1.5% of the upper limit of the range of volumetric flowrate.
The float height h corresponding to each flow points were determined by real flow experiment.

5. CFD Numerical Computation

In 1992, CFD method was firstly introduced into the study of glass tube rotameter by Buckle and Durst etc, and the advanced Laser Doppler Velocimetry was used for experimental test. The results showed good agreement between the data of experiment and simulation [3,4]。 In this study, The CFD method was employed to compute the four types of DN100 mental tube orifice rotameter.

5.1 Meshing the Model

The roles of the guide frame of the rotameter are as follows. The one is to restrict the location of the float when it moves up and down. And second, to prevent the float from hitting the wall. For numerical calculation models of the internal fluid field consistent with the actual fluid field to the full, the numerical computation model of rotameter with the upper and lower guide frame was created. Fig.5 shows the geometry model of orifice rotameter created in the CFD pre-processing software 'GAMBIT'. The positive X direction is the flow direction of fluid. In order to guarantee the fluid state of the entrance face and exit face of rotameter fully developed, the additional 200 mm entrance straight pipe and 500 mm exit straight pipe were created. The diameter of the entrance straight pipe and exit straight pipe is 100 mm.

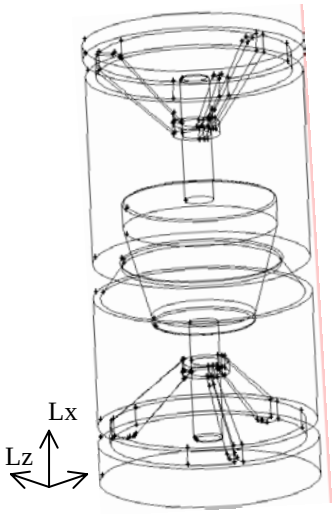

Fig.5 Simulation model of orifice-type rotameter

After creating the geometry model in GAMBIT, the mesh information was exported into commercial CFD software 'FLUENT' for calculation. The whole fluid field is divided into interconnected three portions, the entrance section, rotameter and exit section, so that fine meshing could be provided for efficient computing. The 'GAMBIT' commands Size Functions allow you to control the size of the mesh in regions surrounding a specified entity. A size function attaches to the geometry rotameter and defined with respect to the faces of cone tube, float and guide rods was created. The initial value of mesh-element is set to 1.5 mm, the maximum mesh-element edge lengths set to 3 mm, growth rate set to 1.05 [5]. As the complexity and irregular of the internal structure of rotameter, the fluid domain of rotameter was discretized using T-grid and Cooper option of the software 'GAMBIT'. To control the total number of meshing elements, the fluid domains of the entrance straight pipe and exit straight pipe were discretized using hexahedral mesh.

5.2 Computational Conditions

'FLUENT' has been used for analyzing fluid flow problems involving complex geometries. By the diameter of rotameter, the measured medium and measuring range, the analyzed fluid domain is turbulence [6]. To solve practical engineering problems by turbulence models, the method of simple, practical and high accuracy is the standard k-ε model. Steady solver was chosen. Standard

k-ε two-equation viscosity model was selected turbulence center zone. And non-equilibrium wall function method was used near wall. The employed numerical scheme belongs to a finite volume group and adopts integral form of the conservation equations. The solution domain is subdivided into a finite number of contiguous control volumes and conservation equations are applied to each control volume [7].

Fluid is water at 20 ℃. Its density is 998.2kg/m^3 and its viscosity is 1.003 × 10^{-3}kg/m·s. The velocity at the inlet and outflow at the outlet were specified as the boundary conditions for the geometry considered. In velocity boundary condition, the default value of turbulence intensity and hydraulic diameter was specified as the turbulence parameters, where hydraulic diameter was the diameter of entrance straight pipe. Respectively, wall roughness height of wall roughness is set to 0.04 mm and roughness constant of wall roughness is set to 0.6. In solution control parameters, the discrete format is specified as 'Coupled' algorithm based on pressure-velocity coupling and the pressure equation was specified as the first-order standard format. Other equations were specified as second order upwind scheme.

5.3 Results and Discussions

Corresponding to the float height *h* in Table 3, 5 numerical computation models of 4 different orifice rotameters as shown in Figure 3 were established, respectively.

5.3.1 Flowrate Data and Analysis

The guide bars of rotameter were installed on the upper surface and lower surface of the float. The float reaches to a height *h* in the tube where weight *G* of the float and guide bars is balanced by the lift force F_S. While 'FLUENT' start computing, residuals and F_S were monitored. When the residuals converged to 10^{-4} and the lift coefficient of C_d did not change, the calculation is ended. The error analysis method of the float forced balance, which controls the computational precision, was adopted to adjust the inlet flowrate. When the relative error of F_S and *G* is less than 0.2%, the inlet flowrate was adopted as simulation flowrate. The data were shown in Table 4, where q_S is the simulation flowrate and k_S is linearity computed from Equation (3) 。

Table.4 Comparing of simulation data

h/ mm	Orifice100		Orifice100-1		Orifice100-2		Orifice100-3	
	q_S/(m^3/h)	k_S/ %	q_S/(m^3/h)	k_S/ %	q_S/(m^3/h)	k_S/ %	q_S/(m^3/h)	k_S/ %
4.2	6.183		6.620		5.772		6.433	
18.2	19.800		20.912		17.405		21.443	
22.5	24.880	4.76	25.902	3.51	21.253	1.69	27.886	3.27
33.8	41.944		42.245		32.618		45.070	
45.2	59.406		58.053		42.024		60.547	

From Table 3 it can be seen that,

1) Analysis from the flowrate, flowrate of Orifice100-2 is less than that of Orifice100 at different *h.* And the difference increases with the increase of *h*. The flowrate of Orifice100-1 and Orifice100-3 is close to that of Orifice100. When *h* equals 45.2 mm, the simulation flowrate of Orifice100-2 is 17.382m^3/h less than that of Orifice100, significantly reduced the upper limit of flowrate range. The structure of Orifice100-2 is not available.

2) Analysis from the linearity, Orifice100 has the worst linearity of 4.76% and Orifice100-2 has the best linearity of 1.69%. The linearity of Orifice100-1 and Orifice100-3 are middle, and the two values are close.

5.3.2 Pressure Loss Data and Analysis

For the same rotameter, the pressure loss increases with increasing of *h* (increasing of flowrate). So the pressure loss corresponding to the upper limit of the range of volumetric flowrate is characterized by an important indicator of performance of the rotameter.

In addition to Orifice100-2, the simulation data of pressure loss of the other three types when *h* is 45.2mm are shown in table 5. Where, P_{Loss} represents the pressure loss of the orifice rotameter, P_{FLoss} represents the pressure loss between the upper and lower section of float. From Table 5 it can be seen that, Orifice100 has the maximum P_{Loss} and P_{Floss} and Orifice100-3 has the minimum P_{Loss} and P_{Floss}.

When *h* is 45.2mm, Fig.6 shows static pressure distributions of Orifice100, Orifice100-1 and Orifice100-3. It can be seen from Fig.6 that Orifice100 has the maximum pressure gradients and Orifice100-1 has the minimum pressure gradient. Compared with Orifice100-1, the pressure gradient of Orifice100-3 is slightly bigger. But the maximum flowrate of Orifice100-3 is 2.494m^3/h more than Orifice100-1. The cause of the pressure gradient slightly larger is its flowrate slightly bigger.

Table.5 Pressure loss when h=45.2mm

model	q_S/(m^3/h)	P_{Loss} (KPa)	P_{FLoss} (KPa)
Orifice100	59.406	10.4077	8.6030
Orifice100-1	58.053	8.5492	8.0342
Orifice100-3	60.547	10.2053	8.2679

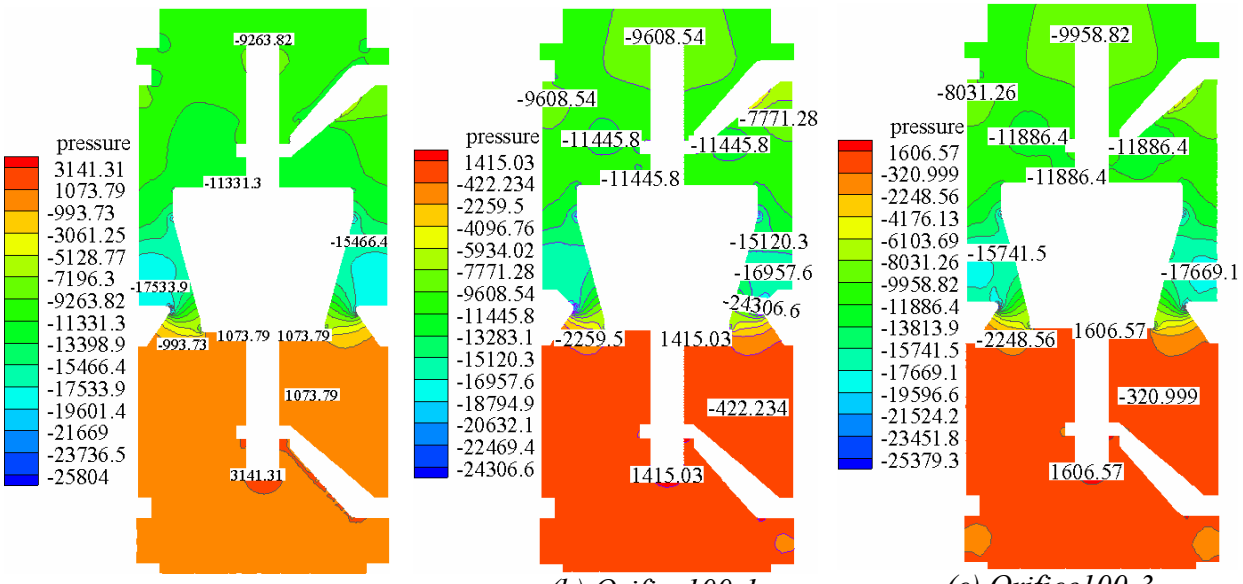

(a) Orifice100 *(b) Orifice100-1* *(c) Orifice100-3*

Fig.6 Static pressure distributions when h=45.2mm

5.3.3 Overall Analysis

From 4.3.1 it can be seen that, although Orifice100-2 has the largest improvement on linearity, but it can not meet the requirement of the upper limit of the range of volumetric flowrate. Comprehensive analysis from the perspective of flow range and linearity, Orifice100-1 and Orifice100-3 were well.

From 4.3.2 it can be seen that, Orifice100-3 has the maximum flowrate. Moreover, its pressure gradient is less than Orifice100. Orifice100-3 can improve the stability of orifice rotameter.

From overall analysis, it can be seen that Orifice100-3 not only improves the linearity and stability, but also meets the requirements of the upper limit of the range of volumetric flowrate.

6 Conclusion

The method of CFD was employed to compare 4 different structural types of orifice rotameter. By analyzing the simulation flowrate and pressure loss, the optimization direction of orifice rotameter had been obtained. To further optimize the structural parameters of Orifice100-3, the performance of orifice rotameter can be improved.

References

[1] Su Yanxun, Liang Guowei, Sheng Jian. Flow measurement and testing [M]. Beijing: China Measurement Press, 2007(in Chinese).
[2] JJG257-2007 Verification regulation of rotameter [S]. 2007.
[3] Bueckle U, Durst F, Melling A. Investigation of a floating element flowmeter [J]. Flow Measurement and Instrumentation, 1992, 3 (4):215-225.
[4] Bueckle U, Durst F, Melling A. Further investigation of a floating element flowmeter [J]. Flow Measurement and Instrumentation, 1995, 6 (1):75-78.
[5] Fluent Inc. Gambit Modeling Guide. Fluent Inc, 2003.
[6] Clement Kleinstreuer. Engineering fluid dynamics: an interdisciplinary systems approach [M]. Cambridge University Press, 1997.
[7] Fluent Inc. Fluent User's Guide. Fluent Inc, 2003.
[8] Xu Ying, Liu Zhengxian, Zhang Tao. Computation of the 3D turbulence flow field of float flowmeter[J]. Journalof Tianjin University, 2004, 37(1): 74-79(in Chinese).
[9] Huang Jinchao, Lin Qingping. Principle and application of rotameters[J]. China Instrumentation, 2005 (4): 54-58(in Chinese).
[10] Piao Li-hua, Zhang Tao, Sun Li-jun. Experimental Research of Rotameter Pressure Loss [J]. Control and Instruments in Chemical Industry, 2010, 37(1): 56-59, 62.
[11] GE Lijun, ZHANG Tao, Ye Jiamin etc. APPLICATION OF SCALARIFORM MULTIPILE HOLE CONDITIONER ON HORIZONTAL ROTAMETER [J]. CHINESE JOURAL OF MECHANICAL ENGINEERING, 2006, Vol.42 No.2: 183-186, 191.